Elastic electron scattering from CO_2

1999 J. Phys. B: At. Mol. Opt. Phys. 32 213

(http://iopscience.iop.org/0953-4075/32/2/006)

J. Phys. B: At. Mol. Opt. Phys. **32** (1999) 213–233. Printed in the UK PII: S0953-4075(99)96685-3

Elastic electron scattering from CO_2

J C Gibson†, M A Green‡, K W Trantham†, S J Buckman†, P J O Teubner‡ and M J Brunger‡

† Atomic and Molecular Physics Laboratories, Research School of Physical Sciences and Engineering, Australian National University, Canberra 0200, ACT, Australia
‡ Physics Department, Flinders University of South Australia, GPO Box 2100, Adelaide 5001, SA, Australia

Received 11 August 1998

Abstract. We present measurements of absolute cross sections for low- and intermediate-energy elastic electron scattering from CO_2, which have been measured independently on different experimental apparatus in two laboratories. The results are compared with a number of previous measurements and calculations. Whilst there are some interesting differences between recent experimental determinations, the largest discrepancies are observed between experiment and contemporary scattering theory at very low energies.

1. Introduction

Carbon dioxide is one of the most important constituents of our atmosphere and it plays a role in gas-discharge-based devices such as the CO_2–N_2 laser. Despite this, there are essentially no contemporary measurements of absolute elastic electron scattering cross sections for CO_2 at energies below about 5 eV, a range which includes the region of influence of the strong $^2\Pi$ shape resonance centred at around 3.8 eV. Similarly, and no doubt related to the lack of experimental information, there are very few theoretical investigations of electron scattering by this important molecule. This situation has been largely addressed by us in an earlier publication (Buckman and Brunger 1997) and we shall not repeat that detail here.

Previous crossed-beam experimental studies on CO_2 include the angular distribution measurements of Shyn *et al* (1978), the absolute differential cross section (DCS) and integral cross section (ICS) measurements of Register *et al* (1980), the low-energy DCS of Kochem *et al* (1985), the intermediate energy DCS of Kanik *et al* (1989), the elastic excitation function measurements of Johnstone *et al* (1993) and the very recent DCS and ICS studies of Tanaka *et al* (1998). There have also been a number of electron-swarm-based measurements of the momentum transfer cross section (Lowke *et al* 1973, Nakamura 1995). In general, the level of overlap between the crossed-beam experiments in terms of the incident energies studied is relatively small and, where it exists, the agreement between the measured cross sections is marginal, with the possible exception of the higher energies (> 20 eV).

The range of theoretical activity for this molecule is even less. Morrison and co-workers (Morrison *et al* 1977) performed the first close-coupling calculations and it is only recently that other close-coupling calculations have followed these (Takekawa and Itikawa 1996, Gianturco and Stoecklin 1996, 1997, Lee *et al* 1998). These most recent studies have used model local exchange and polarization potentials in the fixed-nuclei expansion with a multicentred wavefunction (Takekawa and Itikawa 1996), *ab initio* static exchange and static exchange plus

polarization methods with a single-centre expansion (Gianturco and Stoecklin 1996, 1997) and the Schwinger multichannel approach at the static exchange (SMC-SE) level (Lee *et al* 1998).

The present measurements were undertaken specifically to address the need for contemporary absolute scattering cross section measurements for CO_2 at low incident electron energies. We have carried out these measurements in two laboratories on different scattering apparatus. Both sets of measurements use the relative flow technique (Srivastava *et al* 1975) in order to normalize the relative angular distributions. The measurements from the two spectrometers cover different energy ranges: the ANU (Australian National University) apparatus has been used for the region 1–10 eV, whilst the Flinders University apparatus has covered the energy range 5–50 eV. The measurements overlap at two energies, 5 and 10 eV, to enable direct comparison with one another.

The details of the experimental apparatus and techniques are covered in the next section. Following that the results are presented and discussed in section 3, where they are also compared with previous experiment and theory. Some final observations and conclusions are then made.

2. Experimental considerations

The electron spectrometers used for the present measurements are both based around conventional electrostatic hemispherical analysers and electron optics. They have been described in detail previously (Gulley *et al* 1993, Brunger and Teubner 1990) and that detail will not be repeated here. However, it is relevant to provide some details of the relative flow technique and to note some small differences in its application between the two laboratories.

The differential cross section for an elastic collision of an electron of energy E with an atom or molecule is given by

$$\frac{\mathrm{d}\sigma}{\mathrm{d}\Omega}(E,\theta) = \frac{I_\mathrm{s}(E,\theta)}{I_0 N (l\,\Delta\Omega)\varepsilon\tau} \tag{1}$$

where θ is the electron scattering angle, N is the gas number density, I_0 and I_s are the incident and scattered electron currents, respectively, l is the length of the interaction region, $\Delta\Omega$ is the solid angle subtended by the interaction volume at the detector and τ is the transmission of the scattered electron analyser and ε is the efficiency of the electron detector. With the exception of the incident and scattered electron currents, the determination of most of the quantities in equation (1) poses severe difficulties for absolute measurements and the uncertainties which are involved in their determination can be substantial. As a result, most workers in the field use some alternative technique for normalizing their relative angular distribution measurements.

The relative flow technique, developed at JPL by Trajmar and colleagues (see, for example, Srivastava *et al* 1975, Nickel *et al* 1989), has become more or less the standard means by which electron scattering cross sections are placed on an absolute scale. The technique is conceptually simple, relying on relatively straightforward measurements of the ratio of scattered electron intensities for the gas of interest relative to that for a 'standard' gas, which, in most cases, is helium. In this fashion, the need to make difficult, absolute measurements of experimental parameters such as the gas number density or collision volume is obviated, and the results that are obtained from a properly conducted relative flow experiment can, in principle, provide more accurate results than fully absolute measurements. However, there are many conditions that need to be fulfilled for a properly conducted relative flow experiment. These have been discussed in some detail in a number of recent papers (e.g. Nickel *et al* 1989, Buckman *et al* 1993, Buckman and Brunger 1997, Sugara and Boesten 1998) and we do not repeat those discussions here. However, the critical issues in the application of the RFT are related to the

magnitude of the driving pressure of each gas behind the beam-forming device. It is generally accepted that these pressures should be such that the mean free paths for each gas in this region are equivalent, and also that the absolute values of the driving pressures should be low enough that collisions in the gas beam do not significantly affect the shape of the beams in the electron collision region.

Under these circumstances, the DCS for the gas under study can be expressed in terms of that for the standard gas as

$$\frac{\mathrm{d}\sigma}{\mathrm{d}\Omega}(E,\theta)_{\mathrm{T}} = \frac{I_0(\mathrm{He})}{I_0(\mathrm{T})}\frac{N_{\mathrm{e}}(\mathrm{T})}{N_{\mathrm{e}}(\mathrm{He})}\frac{F_{\mathrm{N}}(\mathrm{He})}{F_{\mathrm{N}}(\mathrm{T})}\frac{\mathrm{d}\sigma}{\mathrm{d}\Omega}(E,\theta)_{\mathrm{He}} \tag{2}$$

where I_0 represents the incident electron currents for the target gas and helium, N_{e} the scattered electron count rates for the two gases, F_{N} the normalized relative flow rates for each gas (the measured relative flow rate multiplied by the square root of the molecular mass) and the final term on the right-hand side is the standard cross section for helium at the energy E and angle θ. The normal practice in such experiments is to calibrate the measured flow rates against some readily measurable parameter, such as the driving pressure behind the beam-forming device, as the flow rate itself is difficult to measure with any accuracy during the course of the experiment. Under ideal conditions, the F_{N} for each gas should be identical for any given driving pressure and the ratios of the relative flow rates should be identical to the ratios of the driving pressures. For every gas that we have encountered in our flow rate measurements over the past ten years this, unfortunately, is *not* the case. In all cases, in fact, the ratio of the normalized flow rate for various target gases to that for helium, as a function of driving pressure, differs from unity by between 10–50%. This is the case in both the sets of apparatus that have been used in this study, and it provides a clear indication that it is imperative that the actual flow rates are carefully measured and calibrated against driving pressure for each gas.

The pressure dependence of the relative flow rates for CO_2, for both the ANU and Flinders experiments, are shown in figure 1, together with results for several other gases. Here the raw

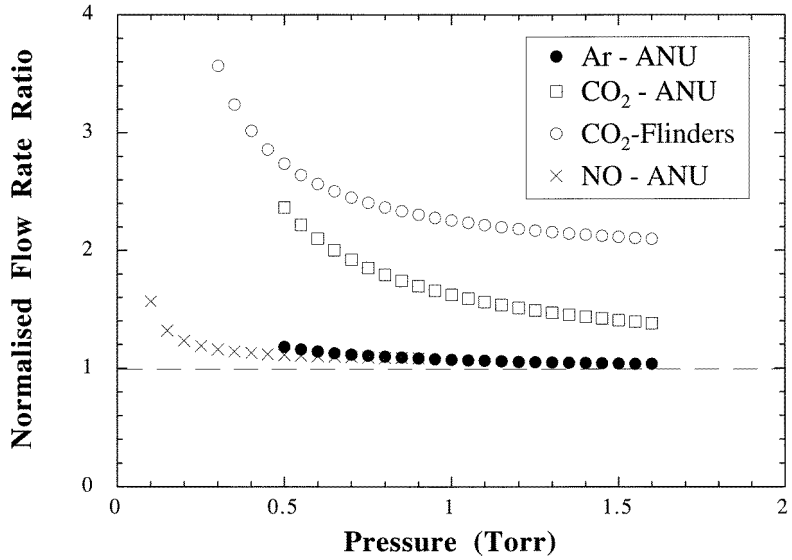

Figure 1. The variation of the ratio of the normalized relative flow rates ($\dot{F}\sqrt{M}$) for a number of gases to that of helium, measured on both the ANU and Flinders spectrometers (see text for details). The response for an 'ideal' gas is indicated by the horizontal broken line.

flow rate data have been converted to normalized flow rates by multiplying each by the square root of the molecular mass, and then they are expressed as a ratio of the normalized flow rate for CO_2 to that for He, as a function of driving pressure, to enable us to display them on the one curve. As we have stated above, for an ideal gas, one would expect such a plot to reveal a horizontal line with a value of unity. This is clearly not the case for the gases shown in the figure, although the results for argon (Ar) and nitric oxide (NO) are more typical of the results for the majority of gases we have studied in this fashion (see also Buckman *et al* 1993). The results for CO_2, however, are quite different. Not only is the ratio substantially larger than unity at all driving pressures, but it is clearly also substantially larger than that found for Ar and NO. The reasons for these differences are not understood, however, they occur in both the Flinders and ANU spectrometers. There are differences in the magnitude of the departure from unity between the two spectrometers which may be attributable to the use of different beam-forming devices. In the ANU spectrometer a multicapillary array, consisting of approximately 280 capillaries, each 40 μm in diameter and 1 mm long, is used, whilst in the Flinders apparatus a single capillary of 0.6 mm diameter and 40 mm long is used. Observations such as those in figure 1 may well be apparatus specific. Nonetheless, these unexpected results may have significant ramifications for the determination of absolute scattering cross sections via the relative flow technique if accurate measurements of the flow rates are not made.

In addition to the abnormally high values of the flow rate ratios for CO_2/He shown in figure 1, we have also noted some other unusual behaviour which results from the admission of CO_2 to either apparatus. Specifically, we initially found a substantial time dependence in the measured CO_2 flow rates which persisted for several days. This we can only attribute to passivation of the surfaces of the gas handling systems although this is surprising, given that they consist of baked, UHV compatible materials.

For the present measurements we have determined the appropriate driving pressures by matching the mean free paths, calculated using the expression

$$\lambda = \frac{1}{\sqrt{2}\,\pi N \delta^2} = \frac{kT}{\sqrt{2}\,\pi P \delta^2} \tag{3}$$

where N is the gas number density, k is Boltzmann's constant, T is the gas temperature in kelvin, P is the gas pressure and δ is the hard-sphere diameter. In addition to matching the mean free paths for the two gases, we also require, based on measurements of the effect of collisions on molecular beam profiles (Buckman *et al* 1993) that the mean free path of each gas is greater than twice the diameter of the capillary array tubes. However, the determination of the required pressures poses some problems as the literature bristles with values of the hard-sphere diameters, and with other parameters from which these can be calculated, for both He and CO_2. Indeed, the very notion of a molecular hard-sphere diameter, whilst conceptually convenient, is somewhat ambiguous for all but a few highly symmetric molecules such as CH_4 (T_d point group symmetry). Thus, even though tables of hard-sphere diameters can be found in the literature, it is quite apparent that there are significant differences in the quoted values for a given species. In particular, variations of up to 45% in the value of δ can be found depending on what type of experimental data was originally used in deriving them. For instance Glasstone (1955) notes the following values of the hard-sphere collision diameter for CO_2; $\delta_{CO_2} = 3.24$ Å, derived from van der Waals constant; $\delta_{CO_2} = 3.60$ Å, derived from viscosity data; $\delta_{CO_2} = 4.38$ Å, derived from diffusion data and $\delta_{CO_2} = 4.82$ Å, as derived from heat conductivity data. Alternatively, if one consults Hirschfelder *et al* (1954) we find hard-sphere diameters $\delta_{CO_2} = 3.996$ or 3.897 Å from viscosity data, and $\delta_{CO_2} = 4.486$ or 4.07 Å on the basis of second virial coefficient data. The CRC handbook

(Weast 1980) quotes $\delta_{CO_2} = 3.23$ Å. In addition, some texts prefer to quote the Lennard-Jones potential (Reif 1965, Reid *et al* 1987) parameter R_0, rather than δ, which can lead to some confusion.

A similar situation, although with less severe variation, can be found in the values for δ_{He}. In this case, most of the values in the literature for δ_{He} appear to lie in the range 2.15–2.65 Å. It is obvious from equation (3) that, depending on the values of δ_{CO_2} and δ_{He} used, the ratio of the driving pressures can vary from between about 1.5–4.5, a quite significant difference. Under these circumstances the actual (optimum) pressure ratio that should be used, to ensure that the mean free path matching criterion is met, becomes topical and, in our view, best addressed by investigating the sensitivity of the measured absolute elastic cross sections to the pressure ratio.

We previously investigated this effect in detail in our methane studies (Bundschu *et al* 1997) and found that, whilst there was a dependence of the cross section value on the pressure ratio used, provided one did not radically depart from the optimum pressure ratio the effect was very small. We also investigated whether there was any dependence of the magnitude of the cross section when different values of driving pressure for CH_4 and He were employed to obtain the same (optimum) pressure ratio. In this case the magnitude of the measured DCS, to within the uncertainty on the data, was found to be unchanged, irrespective of the energy or scattering angle at which the measurement was made. A more limited investigation of these effects was also made in the present CO_2 work and, while the results were at times a little ambiguous, the conclusions we drew were consistent with those found earlier in the methane work.

Finally, we note that the present application of the relative flow technique is made at each scattering angle. The gas pressure, electron beam current and the scattered signal rates are measured sequentially at every angle and energy for both gases. Also, in both sets of apparatus, the gas handling system is established such that both gases are always in the chamber at constant (operational) pressure at all times. This minimizes the effect that gas cycling has on the contact potential and the stability of the electron optics.

3. Results and discussion

3.1. Differential scattering

Absolute differential cross sections for elastic scattering from CO_2 have been measured at 12 energies between 1 and 50 eV. The energy resolution used for these measurements was typically in the range 40–60 meV and an example of an energy loss spectrum (taken on the Flinders spectrometer) is shown in figure 2. The cross sections are tabulated in table 1 and selected examples are illustrated and compared with other experiment and theory, where available, in figures 3–6.

In figure 3(*a*) we show the lowest energy measurement in the present study: the elastic DCS at 1.0 eV. We see the DCS increasing rather rapidly with decreasing scattering angle, a trend which is somewhat unexpected given the lack of any permanent dipole interaction in CO_2 and, whilst the quadrupole moment is reasonably large, this would not be expected to manifest itself as strong forward scattering. Two calculations are available at this energy, those of Gianturco and Stoecklin (1996, 1997) and Lee *et al* (1998), and neither bear much resemblance to the experiment. In the former case, a calculation with an increased number of symmetries included (six as opposed to four, not shown in the figure) does not improve the level of agreement. In the latter case, vibrationally induced dipole effects have been allowed for and a new 'polarizing orbital' scheme has been used. In figure 3(*b*) we show the elastic DCS

Table 1. Absolute differential cross sections (in units of 10^{-16} cm^2 sr^{-1}) for elastic electron scattering from CO_2. The figures in parentheses indicate the absolute uncertainties expressed as a percentage. Integral elastic (Q_e) and elastic momentum transfer (Q_m) cross sections are given at the foot of each column and the uncertainty in these values is estimated to be ±25%.

	Incident energy (eV)							
Angle (deg)	1.0	2.0	3.0	3.8	4.0	4.5	5.0 (ANU)	5.0 (Flind.)
15	1.519 (7.9)	1.244 (44)	0.923 (17)	1.665 (7.7)	1.613 (6.3)	0.864 (8.0)	0.692 (6.5)	—
20	1.288 (9.9)	0.847 (7.3)	0.616 (7.1)	1.307 (7.4)	1.355 (6.4)	0.776 (6.6)	0.645 (6.4)	0.628 (9.6)
30	0.860 (6.8)	0.465 (6.7)	0.342 (6.7)	0.860 (7.2)	0.968 (8.0)	0.692 (6.6)	0.620 (6.6)	0.619 (9.6)
40	0.631 (7.1)	0.282 (6.6)	0.237 (6.3)	0.621 (7.1)	0.751 (6.4)	0.636 (6.4)	0.635 (6.8)	0.681 (9.6)
50	0.477 (7.8)	0.219 (6.6)	0.239 (7.1)	0.553 (7.8)	0.637 (7.1)	0.592 (6.4)	0.612 (6.7)	0.670 (9.6)
55	—	0.210 (7.0)	—	—	—	—	—	—
60	0.358 (8.4)	0.202 (7.8)	0.284 (6.7)	0.505 (6.7)	0.543 (6.6)	0.542 (7.0)	0.593 (6.8)	0.641 (9.5)
70	0.295 (9.9)	0.208 (6.9)	0.318 (6.6)	0.462 (8.0)	0.490 (6.5)	0.492 (6.5)	0.533 (6.6)	0.509 (9.5)
80	0.284 (12)	0.214 (7.4)	0.329 (6.7)	0.398 (7.8)	0.409 (7.8)	0.424 (6.8)	0.463 (6.9)	0.447 (9.6)
90	0.253 (14)	0.236 (7.1)	0.341 (6.5)	0.380 (7.1)	0.358 (7.0)	0.331 (6.9)	0.363 (6.6)	0.331 (9.5)
100	0.247 (8.1)	0.241 (7.2)	0.366 (6.6)	0.364 (6.9)	0.329 (6.7)	0.259 (6.6)	0.277 (6.5)	—
110	0.256 (14)	0.254 (7.5)	0.402 (7.0)	0.390 (6.7)	0.323 (6.5)	0.209 (7.2)	0.209 (6.7)	—
120	0.274 (13)	0.291 (7.3)	0.428 (6.3)	0.398 (7.5)	0.332 (8.7)	0.198 (6.6)	0.186 (7.5)	—
130	0.286 (7.0)	0.318 (6.6)	0.438 (6.9)	0.417 (7.2)	0.360 (7.2)	0.238 (7.1)	0.219 (6.8)	—
Q_e	5.1	4.0	4.8	6.6	6.8	5.3	5.3	5.5
Q_m	3.9	3.8	5.0	5.7	5.6	4.4	4.3	—

	Energy (eV)				
Angle (deg)	5.5	6	7	10 (ANU)	10 (Flinders)
10	—	—	—	1.927 (8.3)	—
15	0.654 (6.4)	0.693 (6.6)	0.887 (7.3)	1.718 (7.0)	2.359 (9.2)
20	0.598 (6.3)	0.614 (6.3)	0.778 (8.4)	1.381 (6.8)	1.839 (9.3)
30	0.589 (6.6)	0.608 (6.6)	0.712 (7.0)	1.031 (6.5)	1.236 (9.3)
40	0.624 (6.6)	0.639 (6.4)	0.716 (7.0)	0.796 (6.5)	1.022 (9.2)
50	0.636 (6.3)	0.637 (7.2)	0.683 (8.8)	0.636 (6.6)	0.781 (9.4)
60	0.604 (6.5)	0.624 (6.4)	0.617 (7.6)	0.542 (6.6)	0.599 (9.2)
70	0.555 (6.5)	0.552 (6.3)	0.554 (6.5)	0.466 (6.9)	0.521 (9.2)
80	0.476 (6.5)	0.496 (6.7)	0.462 (6.9)	0.429 (6.8)	0.452 (9.3)
90	0.394 (6.3)	0.405 (6.4)	0.387 (7.5)	0.394 (6.7)	0.416 (9.1)
100	0.295 (6.8)	0.312 (7.0)	0.326 (6.4)	0.379 (7.0)	—
110	0.229 (6.6)	0.253 (6.7)	0.272 (6.6)	0.395 (6.8)	—
120	0.211 (6.6)	0.237 (6.3)	0.277 (7.6)	0.490 (6.8)	—
130	0.241 (6.6)	0.271 (6.6)	0.325 (7.4)	0.649 (7.1)	—
Q_e	5.4	5.7	6.1	8.5	9.0
Q_m	4.5	4.8	5.2	8.5	—

	Energy (eV)			
Angle (deg)	20	30	40	50
10	8.043 (9.1)	12.16 (5.8)	10.8 (5.8)	10.57 (9.3)
20	4.575 (9.1)	6.469 (5.9)	5.224 (5.9)	4.419 (9.3)
30	2.869 (9.2)	2.724 (6.0)	2.138 (6.1)	1.811 (9.3)
40	1.791 (9.1)	1.361 (6.1)	0.994 (6.0)	0.852 (9.3)
50	1.009 (9.3)	0.786 (6.1)	0.466 (6.8)	0.430 (9.3)
60	0.616 (9.3)	0.468 (6.5)	0.311 (8.1)	0.231 (9.4)
70	0.433 (9.3)	0.313 (6.8)	0.182 (8.7)	0.155 (9.4)
80	0.315 (9.3)	0.23 (6.6)	0.142 (10)	0.128 (9.4)
90	0.296 (9.4)	0.222 (6.7)	0.142 (13)	0.092 (9.4)
Q_e	11.7	12.0	9.5	8.7

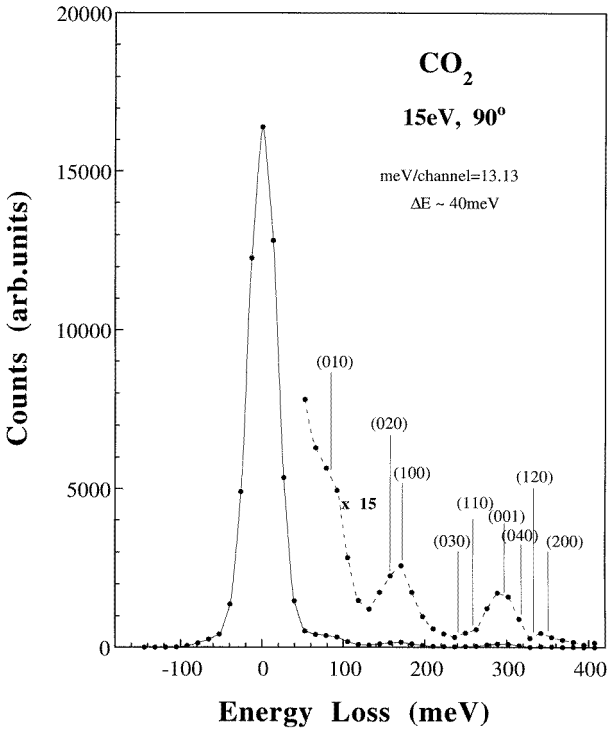

Figure 2. Typical energy-loss spectrum for $e^- + CO_2$ scattering. The present data (●) and an interpolation through those data (——) are shown. The incident electron energy was 15 eV and the electron scattering angle was 90°. The positions of excited vibrational quanta are indicated on the figure.

at an energy of 2 eV. Here we can compare with the very recent measurements of Tanaka *et al* (1998) and, whilst we see that there are some differences in absolute magnitude between the two measurements, for example, about 30% at backward scattering angles, the general trends observed in the DCS are similar. In particular, we see once again that the sharp increase in the DCS at forward angles is evident in both measurements. Three calculations are also shown at this energy. The single-centre-expansion calculation of Gianturco and Stoecklin shows slightly better agreement with experiment than at 1 eV, whilst the calculation of Takekawa and Itikawa (1996) indicates rather good accord with experiment at forward angles, but shows little similarity for angles larger than about 30°. In particular, this calculation predicts a shallow minimum in the DCS at 40° which is not observed in either experimental cross section. Finally, the SMC-SE calculation of Lee *et al* shows a reasonable accord with experiment, particularly that of Tanaka *et al*, at angles greater than 60°, but it also fails to predict the forward angle behaviour correctly.

At 3 eV (figure 3(*c*)), the present data are once again slightly lower (20–30%) than those of Tanaka *et al* across the entire angular range which may be indicative of a normalization difference between the two data sets. The agreement in the shape of the DCS is excellent with both experiments indicating a step-like rise in the cross section at backward angles. At this energy there is an additional experimental measurement by Shyn *et al* (1978) with which to compare. As this measurement is a relative angular distribution we have normalized it to the present data at a scattering angle of 90° and the resulting comparison at other angles

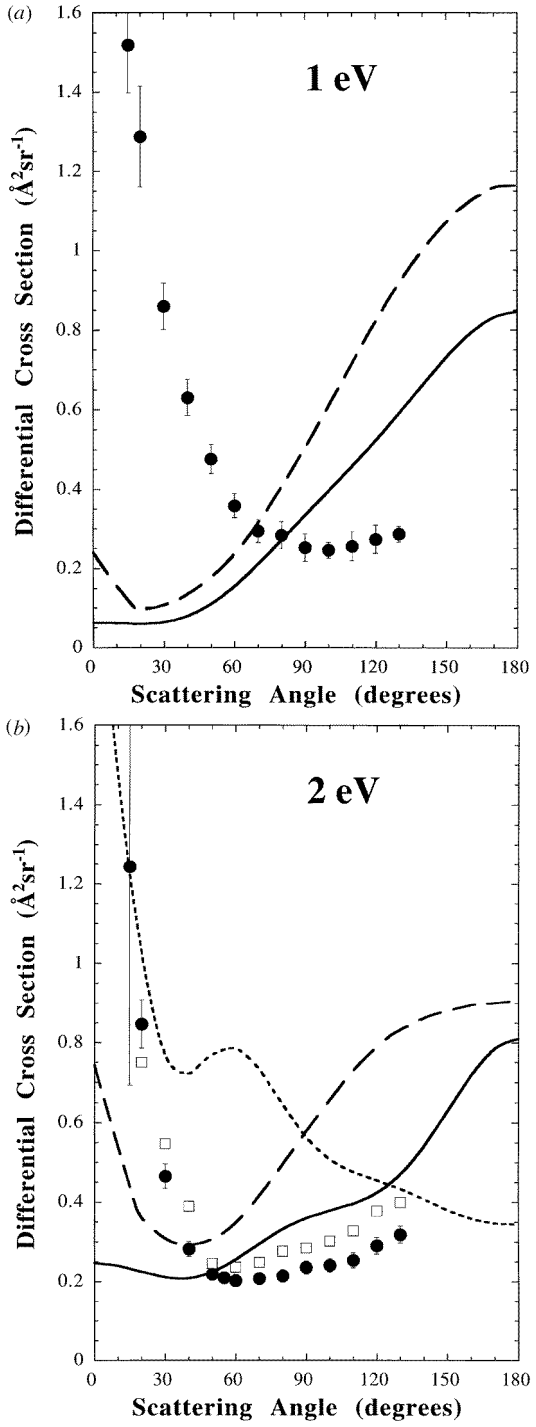

Figure 3. Absolute differential cross sections for elastic electron scattering from CO_2 (in units of 10^{-16} cm^2 sr^{-1}) at energies of (*a*) 1 eV, (*b*) 2 eV, (*c*) 3 eV and (*d*) 3.8 eV. ●, present results (ANU); ×, Shyn *et al*; □, Tanaka *et al*; – – –, Gianturco and Stoecklin; - - - -, Takekawa and Itikawa; ——, Lee *et al*.

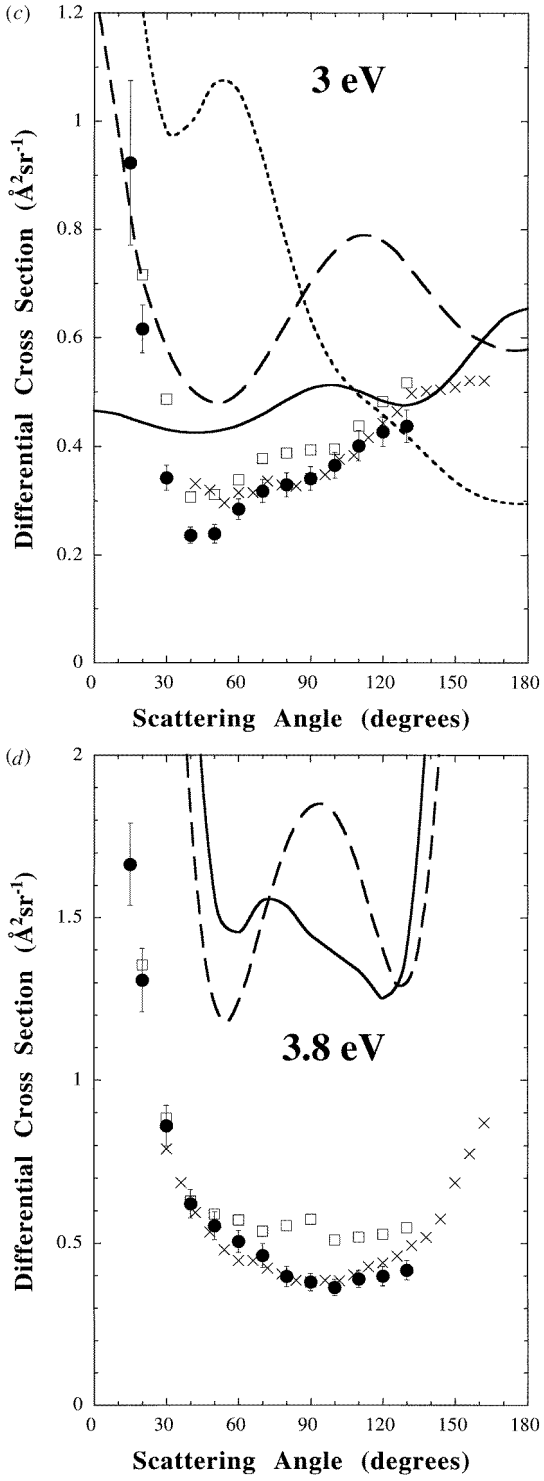

Figure 3. Continued.

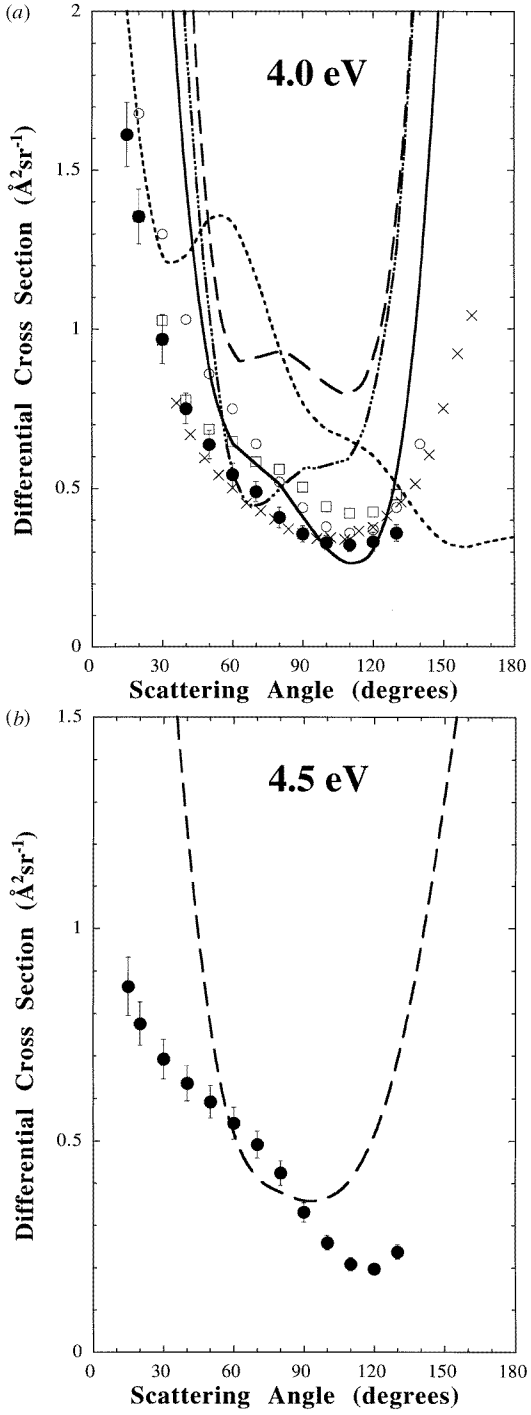

Figure 4. Absolute differential cross sections for elastic electron scattering from CO_2 (in units of 10^{-16} cm^2 sr^{-1}) at energies of (*a*) 4 eV, (*b*) 4.5 eV, (*c*) 5 eV and (*d*) 5.5 eV. ●, present results (ANU); ♦, present results (Flinders); ×, Shyn *et al*; ○, Register *et al*; □, Tanaka *et al*; – · · · –, Morrison *et al*; – – –, Gianturco and Stoecklin; - - - -, Takekawa and Itikawa; ——, Lee *et al*.

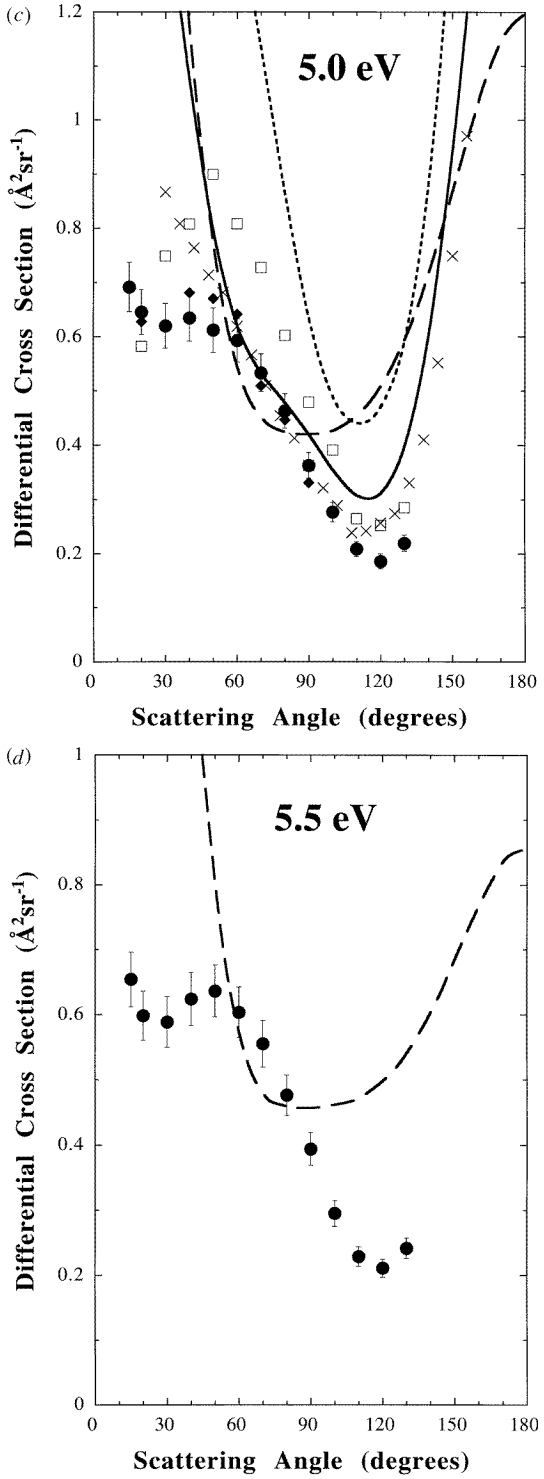

Figure 4. Continued.

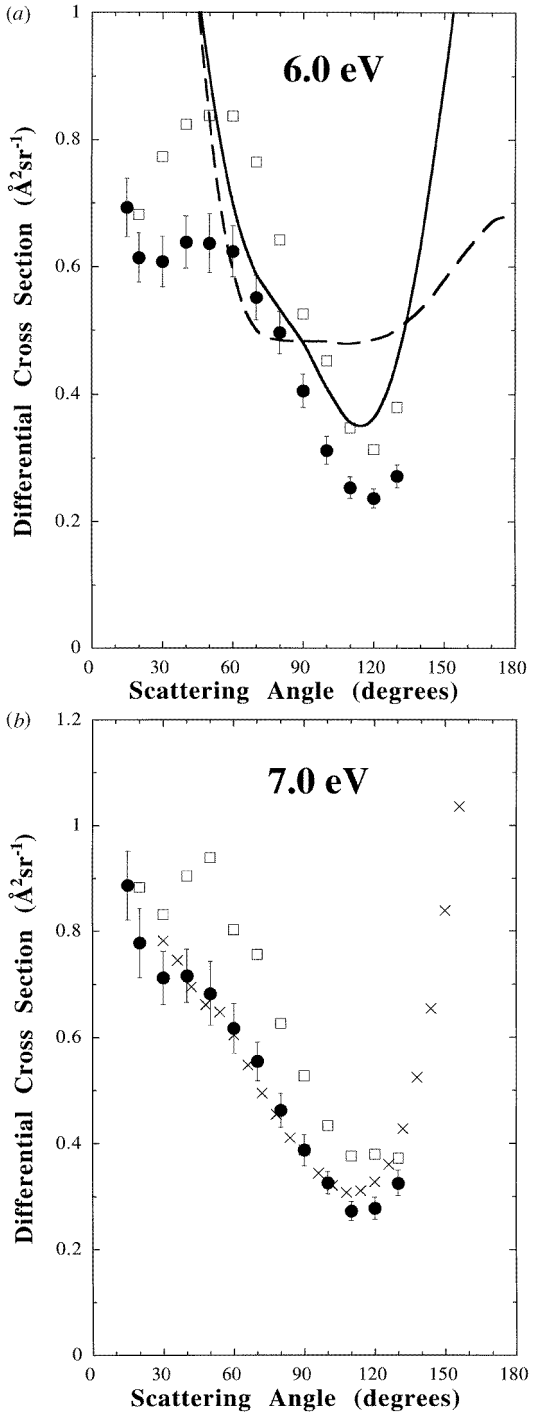

Figure 5. Absolute differential cross sections for elastic electron scattering from CO_2 (in units of 10^{-16} cm^2 sr^{-1}) at energies of (*a*) 6 eV, (*b*) 7 eV, (*c*) 10 eV. ●, present results (ANU); ♦, present results (Flinders); ×, Shyn *et al*; ○, Register *et al*; □, Tanaka *et al*; — · · · —, Morrison *et al*; – – –, Gianturco and Stoecklin; - - - -, Takekawa and Itikawa; ——, Lee *et al*.

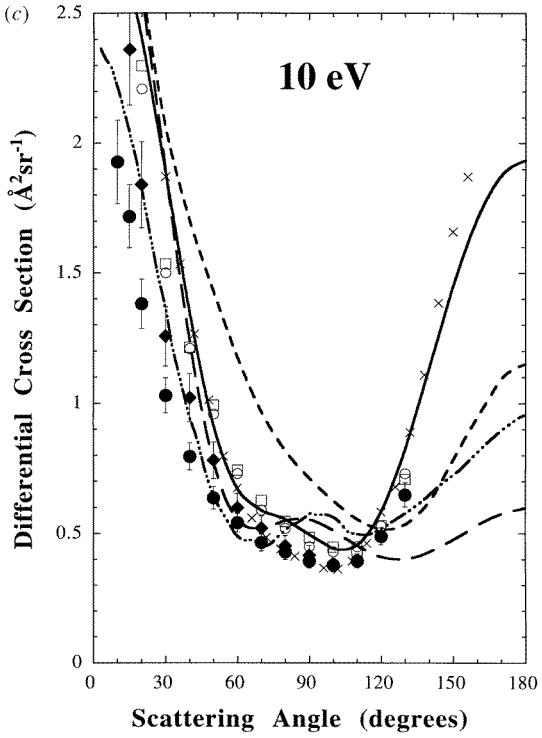

Figure 5. Continued.

shows a good level of agreement in the shape of the two cross sections. The calculations of Gianturco and Stoecklin and Takekawa and Itikawa again show little resemblance in shape to the experimental DCS, although at forward angles the former is in better agreement at this energy than at the lower energies. The calculation of Lee *et al* also bears little resemblance to the experimental DCS. The next measurement, at an energy corresponding to the peak of the low-energy shape resonance at 3.8 eV, is shown in figure 3(*d*). Again, a similar trend is observed within the experimental data sets with the present data, in general, lying below those of Tanaka *et al*. However, this is not true across the whole angular range, indicating some differences in shape between the two DCS. The present data agree well with the shape of the normalized cross section of Shyn *et al*. The theoretical calculations of Gianturco and Stoecklin and Lee *et al* both show a cross section which is considerably larger in magnitude than all the experiments and which exhibits strong minima at mid-angles which are not observed in any of the experimental DCS.

In figure 4 we show a sequence of cross section measurements between 4 and 6 eV at 0.5 eV intervals. At 4.0 eV (figure 4(*a*)), the results are, as expected, similar to those at 3.8 eV, although we have more experimental and theoretical results with which to compare. Once again the level of agreement with the recent data of Tanaka *et al* is mixed. At forward angles ($\leqslant 50^\circ$) the two DCS are in excellent agreement. At larger angles there are again differences of the order of 20–30%, with the present cross section lying below that of Tanaka *et al*. This energy also represents the lowest of a series of absolute DCS measurements by Register *et al* and we see a mixed level of agreement between their DCS and the present across the angular range. For scattering angles above 100° the agreement is very good, whilst at lower scattering

angles their cross section lies above both the present and that of Tanaka *et al* by, at times, 30–40%. Four theoretical curves are shown at this energy, the calculations of Morrison *et al* (1977), Gianturco and Stoecklin (1996, 1997), Takekawa and Itikawa (1996) and Lee *et al* (1998). The best agreement with the experimental data is shown by that of Lee *et al*, although none of the calculations provide an appropriate description of the experimental DCS across the full angular range. At 4.5 eV (figure 4(*b*)) we show the present DCS measurement in comparison with the calculation of Gianturco and Stoecklin. Once again, there are serious discrepancies between theory and experiment. We also note the apparently rapid development of a different shape at forward angles in the experimental DCS. The magnitude of the low-angle cross section has dropped substantially from that at 4 eV and a slight shoulder appears to be developing in the DCS at angles below about 60°.

At an energy of 5 eV some clear differences emerge between the present measurements and the recent data of Tanaka *et al*. The most obvious of these is the behaviour of the DCS at scattering angles below about 60° where the present data show a shoulder or shallow minimum at around 30°–40° followed by a rise at forward angles. On the other hand, the DCS of Tanaka *et al* shows a peak in the DCS at 60° and a cross section which decreases substantially to their lowest measurement angle of 20°. In addition the magnitude of the two DCS at 60° differs by about 40% and, with the exception of the 20° point, the DCS of Tanaka *et al* is once again larger than the present data at all other angles. On the other hand, the DCS of Shyn *et al*, normalized to the present data at 90°, shows no structure at all in the forward direction. In fact, their cross section increases steadily between 110° and 30°. This energy is also the lowest at which the present data from the Flinders spectrometer are available. It is in excellent accord with the ANU data over the common angular range of 20–90°. Unfortunately, neither the calculation of Gianturco and Stoecklin nor that of Takekawa and Itikawa can provide any guidance in this region, as neither calculation indicates the decrease in the cross section at small angles. At 5.5 eV (figure 4(*d*)) the present data illustrate that the forward angle minimum has become a little deeper.

In figure 5 we show the final three low-energy ($\leqslant 10$ eV) DCS measurements from the present work. At 6 eV (figure 5(*a*)) the present (ANU) data are compared with those of Tanaka *et al* and the comparison reveals similar differences to those seen earlier at 5 eV. At angles between 80° and 130° there is a nearly constant difference of around 30% between the two DCS with the present lying lower in magnitude. Below 80°, the differences increase markedly and there is once again a disparity in shape between the two DCS below about 60°. The minimum observed in the present DCS appears to be becoming shallower with increasing energy. At 7.0 eV (figure 5(*b*)), the minimum at forward angles in the present DCS has essentially disappeared, whilst it has manifested itself in the DCS of Tanaka *et al* at an angle of 30°. At larger angles, the discrepancy in absolute magnitude between the two DCS, which was noted above, still persists and there remains a substantial difference between the two cross sections at an angle of 50°, where Tanaka *et al* find a maximum. At 10 eV (figure 5(*c*)), for scattering angles greater than 60°, the agreement between the ANU and Flinders data is again very good. However, for angles less than 60°, the agreement between them is not as impressive as that found earlier at 5 eV. Indeed, the extent of the discrepancy between the magnitude of the Flinders and ANU results is typically of the order of 22%. This is just outside their combined error limits (see table 1) and it may indicate a systematic uncertainty in the use of the relative flow technique in either or both of the experiments and further emphasizes the extent of the experimental difficulty in meeting all the criteria for the proper application of the relative flow procedure (Brunger and Buckman 1997). Both the present ANU and Flinders DCS tend to be somewhat lower in magnitude than the previous experimental results of Register *et al* (1980) and Tanaka *et al* (1998). Nonetheless, to within

their combined experimental uncertainties, the present Flinders data and those of both Register *et al* and Tanaka *et al* are in fair accord over the common angular range of measurement. Also shown is the relative measurement of Shyn *et al* (1978), which has been normalized to the present ANU data at a scattering angle of 90°. The best agreement between these experiments and theory is probably provided by the Schwinger variational calculation of Lee *et al* (1998). This calculation is in quite good agreement with the DCS of Register *et al* and Tanaka *et al* over most of the angular range, but lies higher than the present measurements. The early calculation of Morrison *et al* (1977) is also shown, and it agrees well with the present data at forward angles, but indicates two shallow minima in the DCS at angles near 60° and 120° which are not observed in any of the experiments. While the result of the single-centre expansion, body-fixed approach of Gianturco and Stoecklin (1996, 1997) is in reasonable agreement with the data of Register *et al* and Tanaka *et al*, for scattering angles less than 80°, it also displays structure at larger angles which is not observed experimentally. The calculation of Takekawa and Itikawa, as reported in Tanaka *et al*, is in poor agreement with all of the experimental DCS.

At 20 eV (figure 6(*a*)), we find the present DCS (Flinders) to be in very good agreement with the earlier JPL data of Register *et al*. The later JPL result of Kanik *et al* (1989) is somewhat more forward peaked than the present measurement and that of Register *et al*, although all three sets of data are in accord for scattering angles greater than 30°. It is also apparent from the figure that the recent 20 eV results of Tanaka *et al* (1998) tend to be systematically larger in magnitude than the present DCS, although to within the uncertainties on the two measurements the shape and magnitude agreement between them is reasonable. Once again, the shape of the measurement of Shyn *et al* (1978) is different to the other available data. In particular, their DCS is significantly larger in magnitude than that found by the other experiments at the more forward and backward scattering angles. At this energy there are three calculations currently available. They are due to Onda and Truhlar (1979), Gianturco and Stoecklin (1997) and Lee *et al* (1998), with each method adopting a different approach to solving the scattering equations. Onda and Truhlar did not employ a fully *ab initio* procedure in their calculation. Consequently, we do not discuss it further, except to note that it overestimates the magnitude of the cross section at both forward and backward angles and does not predict the correct angular position for the minimum in the cross section. The approach of Gianturco and Stoecklin is mentioned above and at this energy it does not reproduce the shape of the experimental DCS. Specifically, it underestimates the magnitude of the DCS at forward angles ($\theta < 40°$), overestimates it at middle angles ($70° < \theta < 120°$) and underestimates it again at scattering angles greater than 120°. The calculation which best reproduces the experimental data is the SMC-SE approach of Lee *et al*. This theory is in good agreement with the present 20 eV elastic DCS for scattering angles below 70°. Thereafter, it slightly overestimates the magnitude of the DCS, although it correctly predicts the position of the minimum in the cross section at about 90°.

In figures 6(*b*)–(*d*) we show the 30, 40 and 50 eV elastic DCS, respectively. There are several features common to each of these plots. Within the experimental uncertainties of each measurement, the present data and that of Kanik *et al* (1989) and Tanaka *et al* (1998) are in reasonable accord across the common angular range of measurement. This quite general statement refers to both the shape and magnitude of the measured DCS. In addition, at 50 eV (see figure 6(*d*)), the present DCS is also in excellent agreement with those of Register *et al* (1980). At 30, 40 and 50 eV only the SMC-SE calculation of Lee *et al* (1998) is available for comparison with the experimental DCS. In each case the level of agreement between it and the available experiments is reasonable. We must note, however, that at 30 and 50 eV the theory predicts structure in the DCS which is not observed in any of the measurements.

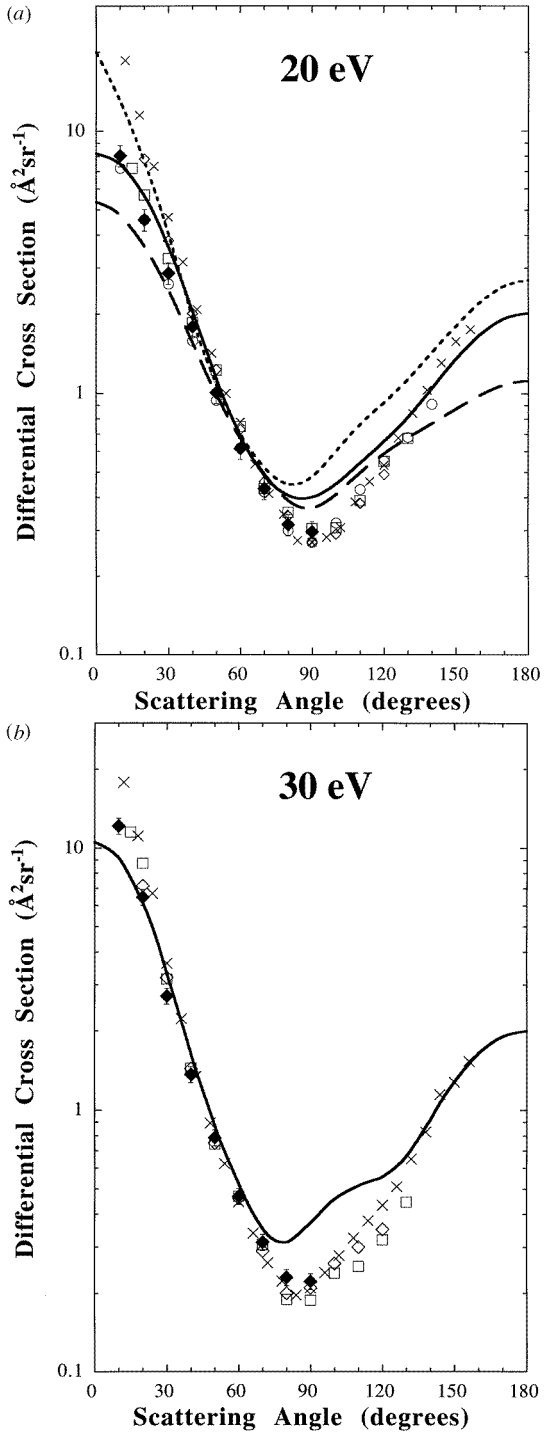

Figure 6. Absolute differential cross sections for elastic electron scattering from CO_2 (in units of 10^{-16} cm^2 sr^{-1}) at energies of (*a*) 20 eV, (*b*) 30 eV, (*c*) 40 eV and (*d*) 50 eV. ♦, present results (Flinders); ×, Shyn *et al*; ○, Register *et al*; □, Tanaka *et al*; ◇, Kanik *et al*; – – –, Gianturco and Stoecklin; - - - -, Onda and Truhlar; ——, Lee *et al*.

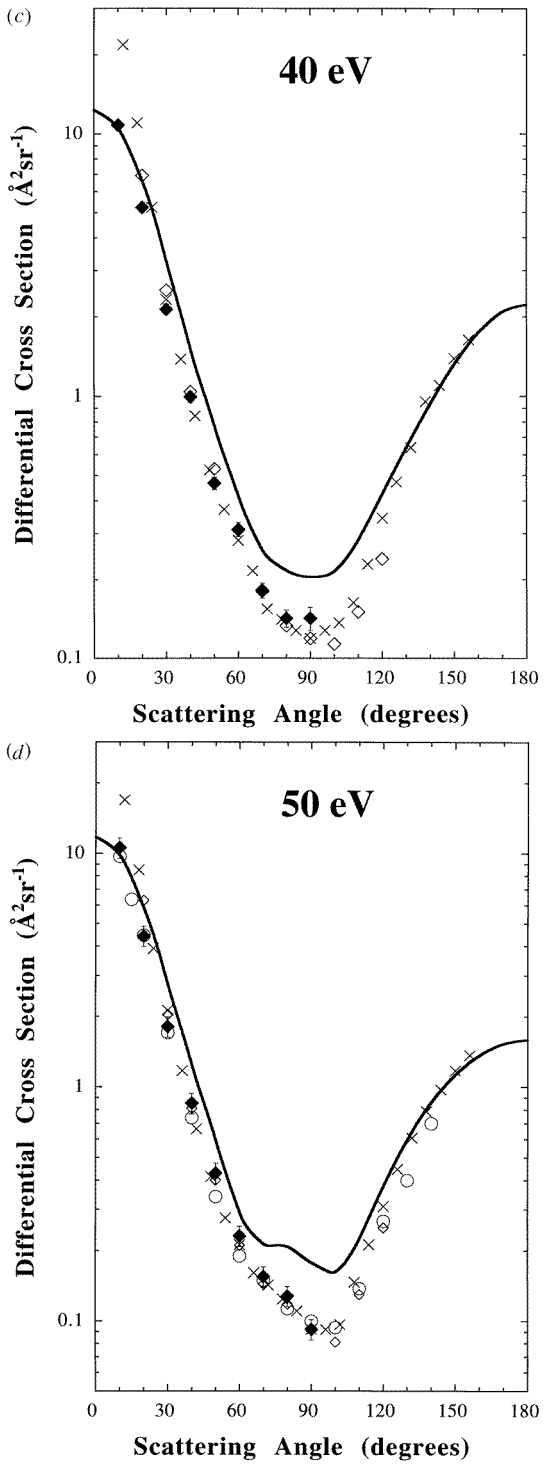

Figure 6. Continued.

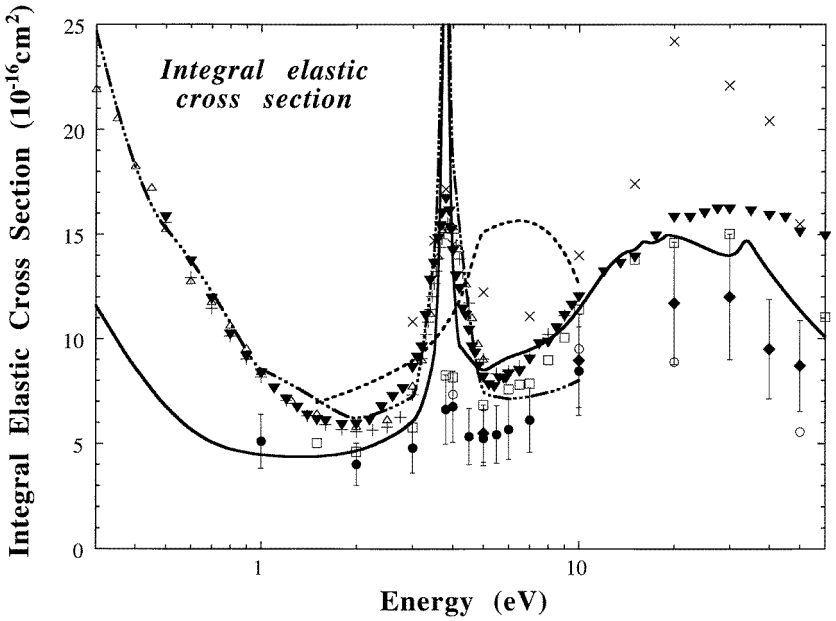

Figure 7. Integral elastic cross sections (in units of 10^{-16} cm^2). ●, present results (ANU); ♦, present results (Flinders); ×, Shyn *et al*; ○, Register *et al*; □, Tanaka *et al*; – · · · –, Morrison *et al*; - - - -, Takekawa and Itikawa; ——, Lee *et al*. Also shown for comparison are the total scattering cross sections of: △, Buckman *et al*; +, Ferch *et al*; and ▼, Szmytkowski *et al*.

3.2. Integral cross sections

Integral elastic and elastic momentum transfer cross sections derived from the present DCS measurements are given in table 1 and presented graphically in figures 7 and 8, respectively. As the angular range of the data from the Flinders spectrometer extends to only 90° we do not derive a momentum transfer cross section from these measurements.

The present integral elastic cross section is shown in figure 7 along with other measurements and calculations, including those for total scattering cross sections. The present measurements are in reasonably good agreement with those of Tanaka *et al* although, as may be expected from the comparisons at the DCS level, the present results are lower in magnitude over most of the energy range. The agreement between the present data and those of Register *et al* is clearly good over the common energy range. As expected, these elastic integral cross sections lie below the total scattering cross sections of, for example, Buckman *et al* (1987), Ferch *et al* (1989) and Szmytkowski *et al* (1987), particularly in the region of the shape resonance, indicating that much of the total cross section in this energy region is due to rotational and vibrational excitation. The Schwinger calculation of Lee *et al* agrees rather well with the present experiment at energies below the resonance, indicating once again how comparisons at the integral cross section level can be misleading. Both the Schwinger calculation and that of Morrison *et al* find the resonance at the correct energy but overestimate the contribution that it makes to the cross section. The calculation of Takekawa and Itikawa (1996) does not reproduce the resonance behaviour or the general energy dependence exhibited in the experimental cross sections.

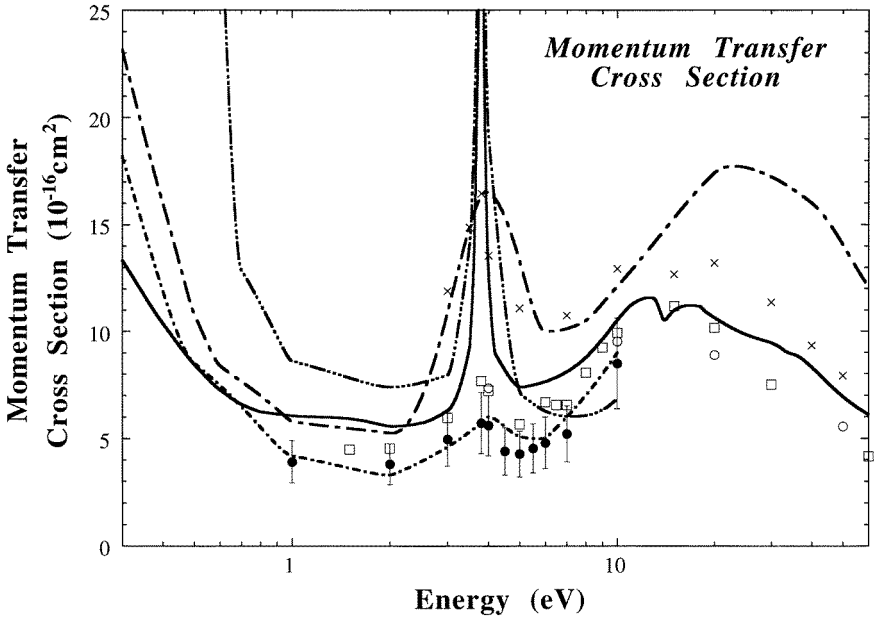

Figure 8. Elastic momentum transfer cross sections (in units of 10^{-16} cm^2). ●, present results (ANU); ×, Shyn *et al*; ○, Register *et al*; □, Tanaka *et al*; – · · · –, Morrison *et al*; ——, Lee *et al*, and the swarm-derived measurements of — - —, Lowke *et al*; and — · —, Nakamura.

The elastic momentum transfer cross section is illustrated in figure 8. Similar comparisons between the experiments and calculations can be drawn to those described above. In addition, we can compare with two swarm-derived cross sections, those of Lowke *et al* (1973) and Nakamura (1995). The former of these is, in fact, a total momentum transfer cross section (i.e. it includes elastic, rotational and vibrational excitation) and, as expected, it is considerably larger in magnitude than the present experimental result. The latter is an elastic momentum transfer cross section and it is in remarkably good agreement with the present cross section.

4. Conclusions

We have presented a body of data for differential elastic electron scattering from CO_2 over a wide range of incident electron energies, spanning the low (1 eV) to intermediate (50 eV) energy regimes. The prime motivation for this work was to provide a set of cross sections at energies below 5 eV where, surprisingly, there was, at the time we commenced the measurements, few data for this important molecule. Whilst the recent measurements by Tanaka *et al* (1998) have alleviated this problem to some extent, the present results largely confirm and extend their results. The most important aspect to emerge from the work of Tanaka *et al* and, in particular, the present work, where we provide more extensive comparisons with contemporary theory, is the poor level of agreement which exists between theory and experiment at energies below about 6 eV. None of the three recent calculations provides a good description of the experimental results at energies below the resonance and, whilst the situation improves marginally with increasing energy, it is only barely satisfactory at an energy of 10 eV. There is a clear need for further theoretical work.

There are also differences between the present experimental results and the recent work of Tanaka *et al* which lie outside the combined experimental uncertainties on the measurements. The general trend which is observed is that there is good agreement in shape between the two DCS at most energies with the present data invariably lying below that of Tanaka *et al*. The exception to this is at energies of around 5 eV, where we see quite different behaviour, particularly at forward angles, in the DCS. In this energy region we also see clear evidence, at forward scattering angles, of behaviour we have observed now in a large number of molecular scattering cross sections, namely a decrease in the DCS at small scattering angles accompanied by the formation of a shallow minimum. This effect has been discussed by us in some detail previously (see, for example, Buckman *et al* 1998) and we shall not repeat that here, other than to note that this apparently ubiquitous behaviour has now been observed in a large number of molecules, diatomic and polyatomic, polar and non-polar, homonuclear and heteronuclear, and it may provide an interesting test bed for theory.

Acknowledgments

It is a pleasure to acknowledge many useful discussions and exchanges of data prior to publication with Mike Morrison, Stephane Mazevet, Lesley Morgan, Franco Gianturco, Thierry Stoecklin, Yukikazu Itikawa, Michiya Takekawa, Chuo-Han Lee, Carl Winstead, Hiroshi Tanaka and Ludwig Boesten. As always we are grateful to the technical staff of our research groups, Stephen Battisson, Kevin Roberts and Greg Hewitt for the construction and maintenance of our apparatus. JG gratefully acknowledges the award of an ANU Graduate School Scholarship and MG an Australian Government Postgraduate Research Award.

References

Brunger M J and Buckman S J1997 *Nucleus* **34** 201
Brunger M J and Teubner P J O 1990 *Phys. Rev.* A **41** 1413
Buckman S J, Elford M T and Newman D S 1987 *J. Phys. B: At. Mol. Phys.* **20** 5175
Buckman S J, Gibson J C and Brunger M J 1998 *Photonic, Electronic and Atomic Collisions* ed F Aumayr and H Winter (Singapore: World Scientific) p 269
Buckman S J, Gulley R J, Moghbelalhossein M and Bennett S J 1993 *Meas. Sci. Technol.* **4** 1143
Bundschu C T, Gibson J C, Gulley R J, Brunger M J, Buckman S J, Sanna N and Gianturco F A 1997 *J. Phys. B: At. Mol. Opt. Phys.* **30** 2239
Ferch J, Masche C, Raith W and Wiemann L 1989 *Phys. Rev.* A **40** 5407
Gianturco F A and Stoecklin T 1996 *J. Phys. B: At. Mol. Opt. Phys.* **29** 3933
——1997 *Phys. Rev.* A **55** 1937
Glasstone S 1955 *Elements of Physical Chemistry* (New York: Van Nostrand)
Gulley R J, Brunger M J and Buckman S J 1993 *J. Phys. B: At. Mol. Opt. Phys.* **26** 2913
Hirschfelder J O, Curtiss C F and Bird R B 1954 *Molecular Theory of Gases and Liquids* (New York: Wiley)
Johnstone W M, Mason N J and Newell W R 1993 *J. Phys. B: At. Mol. Opt. Phys.* **26** L147
Kanik I, McCollum D and Nickel J C 1989 *J. Phys. B: At. Mol. Opt. Phys.* **22** 1225
Kochem K-H, Sohn W, Hebel N, Jung K and Ehrhardt H 1985 *J. Phys. B: At. Mol. Phys.* **18** 4455
Lee C-H, Winstead C and McKoy V 1998 Private communication
Lowke J, Phelps A V and Irwin B W 1973 *J. Appl. Phys.* **44** 4664
Morrison M A, Lane N F and Collins L A 1977 *Phys. Rev.* A **15** 2186
Nakamura Y 1995 *Aust. J. Phys.* **48** 357
Nickel J C, Zetner P W, Shen G and Trajmar S 1989 *J. Phys. E: Sci. Instrum.* **22** 730
Onda K and Truhlar D G 1979 *J. Phys. B: At. Mol. Phys.* **12** 283
Register D F, Nishimura H and Trajmar S 1980 *J. Phys. B: At. Mol. Phys.* **13** 1651
Reid R C, Prausnitz J M and Poling B E 1987 *The Properties of Gases and Liquids* (New York: McGraw-Hill)
Reif F 1965 *Fundamentals of Statistical and Thermal Physics* (New York: McGraw-Hill)
Shyn T W, Sharp W E and Carignan G R 1978 *Phys. Rev.* A **17** 1855

Srivastava S K, Chutjian A and Trajmar S 1975 *J. Chem. Phys.* **63** 2659
Sugara T and Boesten L 1998 *J. Phys. B: At. Mol. Opt. Phys.* **31** 3455
Szmytkowski C, Zecca A, Karwasz G, Oss S, Maciag K, Mannkovic B, Brusa R S and Grisenti R 1987 *J. Phys. B: At. Mol. Phys.* **20** 1987
Takekawa M and Itikawa Y 1996 *J. Phys. B: At. Mol. Opt. Phys.* **29** 4227
Tanaka H, Ishikawa T, Masai T, Sagara T, Boesten L, Takekawa M, Itikawa Y and Kimura M 1998 *Phys. Rev.* A **57** 1798
Weast R C 1980 *Handbook of Chemistry and Physics* 61st edn (Boca Raton, FL: Chemical Rubber Company)